Dialkylaluminium 2-imidazolylphenolates: Synthesis, characterization and ring-opening polymerization behavior towards lactides

Wenjuan Zhang [1], Youhong Wang [1], Lin Wang [1], Carl Redshaw [3,*], and Wen-Hua Sun [1, 2, *]

[1] Key laboratory of Engineering Plastics and Beijing National Laboratory for Molecular Science, Institute of Chemistry, Chinese Academy of Sciences, Beijing 100190, China. zhangwj@iccas.ac.cn; wangyouhong@iccas.ac.cn; wanglin84@iccas.ac.cn, whsun@iccas.ac.cn

[2] State Key Laboratory for Oxo Synthesis and Selective Oxidation, Lanzhou Institute of Chemical Physics, Chinese Academy of Sciences, Lanzhou 730000, China

[3] Department of Chemistry, University of Hull, Hull HU6 7RX, UK. Redshaw@hull.ac.uk

*****Author to whom correspondence should be addressed; E-Mail: whsun@iccas.ac.cn or C.Redshaw@hull.ac.uk; Tel: +86-10-62557955; Fax: +86-10-62618239.

Received: / Accepted: / Published:

Abstract: The stoichiometric reaction of the 2-imidazolylphenols (**L1**–**L9**) with the trialkylaluminium reagents AlR_3 (R = Me, Et and *i*Bu), afforded the corresponding dialkylaluminium 2-imidazolylphenolates [R_2Al(**L1**–**L9**)] (**C1**–**C11**), which were characterized by $^1H/^{13}C$ NMR spectroscopy and by elemental analysis. The molecular structures of the representative complexes **C1**, **C2**, **C4**, **C6** and **C11** were determined by single-crystal X-Ray diffraction, and revealed a distorted tetrahedral geometry at aluminium. The dialkylaluminium 2-imidazolylphenolates (**C1**–**C11**) could efficiently catalyze the ring-opening polymerization of lactides producing high molecular weight polylactide, both in the presence and absence of BnOH, and are rare examples of the use of bi-dentate ligation at aluminium in such lactide polymerization systems. On the basis of the polymerization results for *L*-lactide, *D*-lactide and *rac*-lactide, the nature of the ligands and the Al-alkyls were found to significantly affect the catalytic activity and the properties of the resultant polylactides.

Keywords: Aluminium complexes; 2-imidazolylphenolate; ring-opening polymerization; lactides

1. Introduction

Polylactides (PLAs) have been intensively studied over the past decade due to their favorable biodegradability and biocompatibility for environmental, biomedical, and pharmaceutical applications [1-8]. Lactide exists as three different stereoisomers *L*-lactide, *D*-lactide, and *meso*-lactide, in which equal equivalents of the enantiomers of *L*- and *D*-lactide comprise *rac*-lactide, and this opens the pathway for preparing a range of amorphous to crystalline materials possessing a wide variety of physical, mechanical, and degradable properties. Since *L*-lactic acid is the naturally occurring form, it is much cheaper than *D*-lactide; *meso*-lactide must be separated from the *D*- and *L*-monomers by steam distillation. Most studies have focused on the ring-opening polymerization (ROP) of *L*-lactide and the stereo-selective ROP of *rac*-lactide for crystalline materials because of the limited applications of atactic polymers derived from *rac*-lactide [9-13]. Some aluminium compounds showed good efficiency in the ROP of lactides [14-19], however, some challenges still remain for example, obtaining better efficiency and PLA of higher molecular weight and narrow polydispersity. Important progress was made by Spassky and coworkers, whereby the enantiomerically pure (*R*)-(SalBinap)-AlOMe induced the ROP of *D*-lactide over *L*-lactide, resulting in a tapered stereo-block microstructure [20]. Since then, well-defined metal complexes bearing tetradentate ligands have been intensely explored as efficient initiators in the selective ROP of lactides for precise polylactide architectures either from *rac*-lactide or *meso*-lactide, and several review articles illustrated such progress [21- 25]. In addition, some aluminium complexes ligated by *N,N,O,O*-tetra-dentate salicylaldehyde Schiff-bases could produce highly isotactic polylactides from *rac*-lactide *via* an chain-end-control mechanism [26-29] or site-control mechanism [30-33]. Following on from this, subsequent studies have re-evaluated the Schiff-base aluminium catalytic systems and probed the steric and electronic effects on the polymerization rate and stereo-selectivity [34-35]. In general, most aluminium complexes bearing salicylaldehyde Schiff-bases did not exhibit high efficiency in lactide polymerization, but the achiral Schiff-base aluminium alkoxides showed good stereo-controllability and afforded poly(*rac*-lactide) with a P_m of 90 % and a high T_m of 201 ºC [36-38]. A few papers have reported bi-dentate aluminium complexes for ROP of lactides, [39-43] but with low efficiency and producing polymer of low molecular weight. In contrast, many bi-dentate aluminium complexes have been reported with high efficiency for the ROP of ε-caprolactone (ε-CL) in a well-controlled manner [44-53]. Herein, trials of aluminium imidazolylphenolate complexes with a low-coordination number were deemed worthy of investigation. Importantly, these complexes exhibited good efficiency in the ROP of lactides (*L*-lactide, *D*-lactide and *rac*-lactide), producing polylactides of high molecular weight.

2. Experimental Section

General Considerations. All reactions were performed using standard Schlenk techniques in an atmosphere of high-purity nitrogen or glove-box techniques. Toluene, *n*-heptane and THF were dried by refluxing over sodium and benzophenone, distilled under nitrogen and stored over activated molecular sieves (4Å) for 24 h in a glove-box prior to use. C_6D_6 was dried over activated 4Å

molecular sieves. CH_2Cl_2 and $CDCl_3$ were dried over CaH_2 for 48 h, distilled under nitrogen and stored over activated molecular sieves (4Å) in a glove-box prior to use. $AlMe_3$ were purchased from Aldrich and used as received. Elemental analyses were performed using a PE2400II Series (Perkin-Elmer Co.). ^1H NMR spectra and ^{13}C NMR spectra were recorded on a Bruker DMX-400 (400 MHz for ^1H, 100 MHz for ^{13}C) instrument. All spectra were obtained in the solvent indicated at 25 °C unless otherwise noted and chemical shifts are given in ppm and are referenced to $SiMe_4$ (δ 0.00, ^1H, ^{13}C). The GPC measurements were performed on a set of Water-515 HPLC pumps, a Waters 2414 refractive index detector, and a combination of Styragel HT-2, HT-3 and HT-4, the effective molar mass ranges of which are 100-10000, 500-30000 and 5000-600000, respectively. THF was used as the eluent (flow rate: 1 mL min^{-1}, at 40 °C). Molecular weights and molecular weight distributions were calculated using polystyrenes as standard.

Synthesis of Complexes C1–C11

Dimethylaluminium 2,4-di-*tert*-butyl-6-(4,5-diphenyl-*1H*-imidazol-2-yl)phenolate [Me_2AlL1] (C1). Into a stirred solution of 2,4-di-*tert*-butyl-6-(4,5-diphenyl-1H-imidazol-2-yl)phenol (0.424 g, 1.0 mmol) in toluene (15.0 mL), 1.0 mL (1.0 mmol), $AlMe_3$ solution (1.0 M solution in toluene) was added drop-wise at -30 °C. The slurry was allowed to warm slowly to room temperature and was stirred for 3 h, and the solution became clear. Following concentration to 5 mL *in vacuo*, 10mL *n*-heptane was added, and the solution was placed in the freezer (-30 °C) to afford **C1** as a yellow powder. Yield: 93.8 %. ^1H NMR ($CDCl_3$): 9.34 (s, 1H, N*H*-H), 7.44 (d, 2H, *J* = 2.40, Ar-H), 7.42 (m, 4H, Ar-H), 7.37 (d, 2H, *J* = 1.60, Ar-H), 7.36 (s, 2H, Ar-H), 7.20 (d, 2H, *J* = 2.40, Ar-H), 1.45 (s, 9H, *t*Bu-H), 1.36 (s, 9H, *t*Bu-H), -0.99 (s, 6H, Al(C*H*$_3$)-H). ^{13}C NMR ($CDCl_3$): 157.9, 147.9, 141.2, 138.7, 134.8, 130.8, 130.3, 129.3, 129.2, 128.9, 128.8, 128.5, 127.9, 127.5, 126.8, 117.9, 111.5, 35.6, 34.5, 31.8, 29.6, -9.1. Anal. Calcd for $C_{31}H_{37}AlN_2O$: C 77.47, H 7.76, N 5.83. Found: C 77.31, H 7.83, N 5.75 %.

Diethylaluminium 2,4-di-*tert*-butyl-6-(4,5-diphenyl-*1H*-imidazol-2-yl)phenolate [Et_2AlL1] (C2). The synthesis of **C2** was carried out by the same procedure as that of **C1**, except that $AlEt_3$ was used. Yield: 94.0 %. ^1H NMR ($CDCl_3$): 9.33 (s, 1H, N*H*-H), 7.43 (m, 5H, Ar-H), 7.36 (m, 5H, Ar-H), 7.19 (d, 2H, *J* = 2.4, Ar-H), 1.44 (s, 9H, *t*Bu-H), 1.31 (s, 9H, *t*Bu-H), 0.81 (t, 6H, *J* = 8.4, Al(CH_2CH_3)$_2$-H), -0.34 (m, 4H, Al(CH_2CH_3)$_2$-H)). ^{13}C NMR ($CDCl_3$): 158.6, 148.2, 141.1, 138.5, 134.7, 130.7, 130.2, 129.3, 129.2, 128.9, 128.8, 128.5, 127.9, 127.4, 126.7, 117.8, 111.2, 35.6, 34.4, 31.8, 29.6, 9.1, 0.97. Anal. Calcd for $C_{33}H_{41}AlN_2O$: C 77.92, H 8.12, N 5.51. Found: C 78.12, H 8.05, N 5.39 %.

Diisobutylaluminium 2,4-di-*tert*-butyl-6-(4,5-diphenyl-*1H*-imidazol-2-yl)phenolate [*i*Bu_2AlL1] (C3). The synthesis of **C3** was carried out by the same procedure as that of **C1,** except that *i*Bu_3Al was used. Yield: 83.8 %. ^1H NMR ($CDCl_3$): 9.38 (s, 1H, N*H*-H), 7.45 (m, 5H, Ar-H), 7.35 (m, 5H, Ar-H), 7.20 (d, 2H, *J* = 2.0, Ar-H), 1.64 (m, 2H, Al($CH_2CH(CH_3)_2$)$_2$-H), 1.46 (s, 9H, ^{t}Bu-H), 1.36 (s, 9H, ^{t}Bu-H), 0.76 (m, 12H, Al($CH_2CH(CH_3)_2$)$_2$-H), -0.22 (m, 2H, Al$CH_2CH(CH_3)_2$-H), -0.32 (m, 2H, Al$CH_2CH(CH_3)_2$-H). ^{13}C NMR ($CDCl_3$): 158.2, 148.1, 141.1, 138.5, 134.8, 130.9, 130.5, 129.3, 129.2, 128.8, 128.5, 127.9, 127.5, 126.9, 117.9, 111.3, 35.6, 34.4, 31.8, 29.7, 28.5, 28.1, 26.2, 25.7, 23.4, 19.5. Anal. Calcd for $C_{37}H_{49}AlN_2O$: C 78.68, H 8.74, N 4.96. Found: C 78.55, H 8.83, N 5.02 %.

Dimethylaluminium 2-(4,5-diphenyl-*1H*-imidazol-2-yl)phenolate [Me_2AlL2] (C4). The synthesis of **C4** was carried out by the same procedure as that of **C1**, except that 2-(4,5-diphenyl-1H-imidazol-2-yl)phenol was used. Yield: 91.1 %. ^{1}H NMR ($CDCl_3$): 9.71 (s, 1H, N*H*-H), 7.47 (d, 1H, *J* = 1.6, Ar-H), 7.46 (d, 1H, *J* = 1.6, Ar-H), 7.43 (m, 4H, Ar-H), 7.34 (m, 4H, Ar-H), 6.99 (d, 1H, *J* = 0.8, Ar-H), 6.97 (d, 1H, *J* = 0.8, Ar-H), 6.79 (m, 2H, Ar-H), -0.99 (s, 6H, Al(C*H*$_3$)-H). ^{13}C NMR ($CDCl_3$): 159.3, 147.0, 133.4, 132.0, 131.1, 130.2, 128.5, 128.4, 127.7, 127.5, 126.4, 120.7, 116.7, 114.9, -7.7. Anal. Calcd for $C_{23}H_{21}AlN_2O$: C 74.98, H 5.75, N 7.60. Found: C 75.12, H 5.63, N 7.71 %.

Dimethylaluminium 2-phenoxy-6-(4,5-diphenyl-*1H*-imidazol-2-yl)phenolate [Me_2AlL3] (C5). The synthesis of **C5** was carried out by the same procedure as that of **C1**, except that 2-phenoxy-6-(4,5-diphenyl-1H-imidazol-2-yl)phenol was used. Yield: 89.5 %. ^{1}H NMR ($CDCl_3$): 9.79 (s, 1H, N*H*-H), 7.86 (d, 1H, *J* = 8.2, Ar-H), 7.76 (d, 2H, *J* = 7.2, Ar-H), 7.75 (d, 1H, *J* = 9.2, Ar-H), 7.57 (d, 2H, *J* = 7.6, Ar-H), 7.49 (m, 5H, Ar-H), 7.38 (m, 6H, Ar-H), 7.24 (d, 1H, *J* = 8.2, Ar-H), -0.99 (s, 6H, Al(C*H*$_3$)-H). ^{13}C NMR ($CDCl_3$): 159.1, 146.5, 133.2, 132.8, 131.0, 130.6, 129.5, 129.4, 129.0, 128.8, 128.5, 128.3, 128.0, 127.9, 127.7, 127.2, 126.9, 124.3, 123.1, 122.4, 113.2, -9.3. Anal. Calcd for $C_{29}H_{25}AlN_2O_2$: C 75.64, H 5.47, N 6.08. Found: C 75.56, H 5.53, N 6.16 %.

Dimethylaluminium 5-bromo-2-(4,5-diphenyl-*1H*-imidazol-2-yl)phenolate [Me_2AlL4] (C6). The synthesis of **C6** was carried out by the same procedure as that of **C1**, except that 5-bromo-2-(4,5-diphenyl-1H-imidazol-2-yl)phenol was used. Yield: 83.2 %. ^{1}H NMR($CDCl_3$): 10.82 (s, 1H, N*H*-H), 7.67 (s, 1H, Ar-H), 7.42 (m, 5H, Ar-H), 7.34 (m, 5H, Ar-H), 6.98 (d, 1H, *J* = 8.32, Ar-H), 6.71 (d, 1H, *J* = 7.42, Ar-H), -0.98 (s, 6H, Al(C*H*$_3$)-H). ^{13}C NMR ($CDCl_3$): 153.9, 144.51, 134.5, 133.7, 130.2, 128.5, 127.3, 127.0, 126.9, 126.8, 126.5, 126.4, 126.0, 125.2, 124.1, 115.3, 105.5, -8.7. Anal. Calcd for $C_{23}H_{20}AlBrN_2O$: C 61.76, H 4.51, N 6.26. Found: C 61.59, H 4.45, N 6.38 %.

Dimethylaluminium 2,4-dibromo-6-(4,5-diphenyl -*1H*-imidazol-2-yl)phenolate [Me_2AlL5] (C7). The synthesis of **C7** was carried out by the same procedure as that of **C1**, except that 2,4-dibromo-6-(4,5-diphenyl-1H-imidazol-2-yl)phenol was used. Yield: 85.8 %. ^{1}H NMR ($CDCl_3$): 10.85 (s, 1H, N*H*-H), 7.61 (s, 1H, Ar-H), 7.39 (m, 4H, Ar-H), 7.31 (m, 5H, Ar-H), 6.99 (d, 1H, *J* = 8.32, Ar-H), 6.75 (d, 1H, *J* = 7.42, Ar-H), -0.95 (s, 6H, Al(C*H*$_3$)-H). ^{13}C NMR ($CDCl_3$): 153.6, 144.5, 134.8, 133.4, 130.0, 128.8, 127.5, 127.0, 126.8, 126.7, 126.5, 126.3, 126.2, 125.9, 123.9, 114.9, 106.0, -8.6. Anal. Calcd for $C_{23}H_{19}AlBr_2N_2O$: C 52.50, H 3.64, N 5.32. Found: C 52.61, H 3.56, N 5.28 %.

Dimethylaluminium 1-(4,5-diphenyl-*1H*-imidazol-2-yl)naphthalen-2-olate [Me_2AlL6] (C8). The synthesis of **C8** was carried out by the same procedure as that of **C1**, except that 1-(4,5-diphenyl-1H-imidazol-2-yl)naphthalen-2-ol was used. Yield: 90.2 %. ^{1}H NMR ($CDCl_3$): 9.87 (s, 1H, N*H*-H), 8.09 (d, 1H, *J* = 8.4, Ar-H), 7.84 (d, 1H, *J* = 8.0, Ar-H), 7.79 (d, 1H, *J* = 9.2, Ar-H), 7.52 (d, 1H, *J* = 7.2, Ar-H), 7.46 (m, 5H, Ar-H), 7.36 (m, 6H, Ar-H), 7.22 (d, 1H, *J* = 8.8, Ar-H), -1.01 (s, 6H, Al(C*H*$_3$)-H). ^{13}C NMR ($CDCl_3$): 159.8, 146.1, 133.6, 132.2, 131.4, 130.1, 129.5, 129.0, 128.3, 128.2, 128.0, 127.8, 127.5, 127.4, 126.6, 124.0, 123.5, 122.1, 113.8, -9.6. Anal. Calcd for $C_{27}H_{23}AlN_2O$: C 77.49, H 5.54, N 6.69. Found: C 77.53, H 5.45, N 6.71 %.

Dimethylaluminium 2,4-di-*tert*-butyl-6-(*1H*-phenanthro[9,10-d]imidazol-2-yl)phenolate [Me_2AlL7] (C9). The synthesis of **C9** was carried out by the same procedure as that of **C1**, except that 2,4-di-*tert*-butyl-6-(1H-phenanthro[9,10-d]imidazol-2-yl)phenol was used. Yield: 93.7 %. ^{1}H NMR ($CDCl_3$): 10.11 (s, 1H, N*H*-H), 8.77 (t, 2H, *J* = 6.8, Ar-H), 8.62 (d, 1H, *J* = 7.6, Ar-H), 8.15 (m, 4H,

Ar-H), 7.76 (t, 2H, *J* = 7.2, Ar-H), 7.71 (m, 2H, Ar-H), 7.53 (d, 2H, *J* = 2.4, Ar-H), 7.40 (d, 2H, *J* = 2.0, Ar-H), 1.52 (s, 9H, ^{t}Bu-H), 1.42 (s, 9H, ^{t}Bu-H), -0.49 (s, 6H, Al(C*H*$_3$)-H). ^{13}C NMR ($CDCl_3$): 158.5, 150.9, 141.3, 139.1, 128.8, 128.7, 127.9, 127.6, 127.4, 127.3, 127.1, 126.7, 126.4, 125.5, 124.2, 124.1, 123.7, 121.4, 120.3, 118.8, 111.4, 35.7, 34.6, 31.8, 29.6, -7.7. Anal. Calcd for $C_{31}H_{35}AlN_2O$: C 77.80, H 7.37, N 5.85. Found: C 77.73, H 7.45, N 5.94 %.

Dimethylaluminium 2,4-di-*tert*-butyl-6-(*1H*-phenanthro[9,10-d]oxazol-2-yl)phenolate [Me$_2$AlL8] (C10). The synthesis of **C10** was carried out by the same procedure as that of **C1**, except that 2,4-di-*tert*-butyl-6-(phenanthro[9,10-d]oxazol-2-yl)phenol was used. Yield: 87.6 %. ^{1}H NMR ($CDCl_3$): ^{1}H NMR ($CDCl_3$): 8.78 (m, 2H, Ar-H), 8.52 (d, 1H, *J* = 7.6, Ar-H), 8.39 (d, 2H, *J* = 8.8, Ar-H), 8.01 (d, 1H, *J* = 2.4, Ar-H), 7.78 (m, 4H, Ar-H), 7.61 (d, 1H, *J* = 2.4, Ar-H), 1.52 (s, 9H, *t*Bu-H), 1.44 (s, 9H, *t*Bu-H), -0.44 (s, 6H, Al(C*H*$_3$)-H). ^{13}C NMR ($CDCl_3$): 165.7, 160.5, 143.7, 140.7, 139.5, 131.1, 129.8, 129.7, 129.6, 128.1, 128.0, 127.8, 127.2, 124.1, 123.9, 122.8, 121.4, 120.9, 119.8, 109.9, 35.6, 34.6, 31.6, 29.6, -7.9. Anal. Calcd for $C_{31}H_{34}AlNO_2$: C 77.64, H 7.15, N 2.92. Found: C 77.80, H 7.06, N 3.01 %.

Dimethylaluminium 2-(*1H*-phenanthro[9,10-d]imidazol-2-yl)phenolate [Me$_2$AlL9] (C11). The synthesis of **C11** was carried out by the same procedure as that of **C1**, except that 2-(1H-phenanthro[9,10-d]imidazol-2-yl)phenol was used. Yield: 85.9 %. ^{1}H NMR ($CDCl_3$): 10.22 (s, 1H, N*H*-H), 8.79 (m, 2H, Ar-H), 8.65 (d, 1H, *J* = 8.0, Ar-H), 8.11 (t, 1H, *J* = 3.2, Ar-H), 7.79 (t, 1H, *J* = 7.6, Ar-H), 7.74 (m, 2H, Ar-H), 7.67 (d, 1H, *J* = 6.8, Ar-H), 7.40 (t, 1H, *J* = 7.2, Ar-H), 7.17 (d, 2H, *J* = 7.2, Ar-H), 7.08 (d, 1H, *J* = 8.8, Ar-H), 6.88 (t, 1H, *J* = 7.6, Ar-H), -0.46 (s, 6H, Al(C*H*$_3$)-H). ^{13}C NMR ($CDCl_3$): 158.6, 150.8, 141.3, 139.3, 128.7, 128.7, 127.9, 127.5, 127.3, 127.1, 127.0, 126.9, 126.2, 125.7, 124.2, 124.0, 123.3, 121.6, 120.3, 118.9, 111.2, -7.9. Anal. Calcd for $C_{23}H_{19}AlN_2O$: C 75.40, H 5.23, N 7.65. Found: C 74.29, H 5.31, N 7.72 %.

Ring-Opening Polymerization (ROP) of *L*-lactide, *D*-lactide, *rac*-lactide (LA) in the presence of BnOH. Typical polymerization procedures in the presence of one equivalent of benzyl alcohol (Table 4, run 1) are as follows. A toluene solution of **C1** (0.010 mmol, 1.0 mL toluene) and BnOH (0.010 mmol) were added into a Schlenk tube in the glove-box at room temperature. The solution was stirred for 2 min, and then *L*-lactide (2.5 mmol) along with 1.5 mL toluene was added to the solution. The reaction mixture was then placed into an oil bath pre-heated at 110 °C, and the solution was stirred for the prescribed time (24 h). The polymerization mixture was then quenched by addition of an excess of glacial acetic acid (0.2 mL) into the solution, and the resultant solution was then poured into methanol (200 mL). The resultant polymer was then collected on filter paper and was dried *in vacuo*.

Ring-opening Polymerization (ROP) of *L*-lactide, *D*-lactide, *rac*-lactide (LA) in the absence of BnOH. Typical polymerization procedures in the absence of benzyl alcohol (run 1, Table 5) are as follows. A toluene solution of **C1** (0.010 mmol, 1.0 mL toluene) was added into a Schlenk tube in the glove-box at room temperature. The solution was stirred for 2 min, and then *L*-lactide (2.5 mmol) along with 1.5 mL toluene was added to the solution. The reaction mixture was then placed into an oil bath pre-heated at 110 °C, and the solution was stirred for the prescribed time (24 h). The polymerization mixture was then quenched by addition of an excess of glacial acetic acid (0.2 mL) into

the solution, and the resultant solution was then poured into methanol (200 mL). The resultant polymer was then collected on filter paper and was dried *in vacuo*.

Crystal Structure Determinations Single crystals of **C1, C2, C4, C6** and **C11** suitable for single crystal X-ray diffraction were obtained from chilled toluene/*n*-heptane solution. With graphite-monochromated Mo K_α radiation (k = 0.71073 Å), cell parameters were obtained by global refinement of the positions of all collected reflections. Intensities were corrected for Lorentz and polarization effects and empirical absorption. The structures were solved by direct methods and refined by full-matrix least squares on F^2. All hydrogen atoms were placed in calculated positions. Structure solution and refinement were performed by using the SHELXL-97 package [54]. Details of the X-ray structure determinations and refinements are provided in Table 1.

Table 1 Crystal Data and Refinement Details for **C1**, **C2**, **C4**, **C6**, and **C11**

	C1	**C2**	**C4**	**C6**	**C11**
Empirical formula	$C_{31}H_{37}AlN_2O$	$C_{33}H_{41}AlN_2O$	$C_{23}H_{21}AlN_2O$	$C_{23}H_{20}AlBrN_2O$	$C_{23}H_{19}AlN_2O$
Formula weight	480.61	508.66	368.40	447.30	366.38
Crystal color	Colorless	Colorless	Colorless	Colorless	Colorless
Temperature (K)	173(2)	172(2)	173(2)	173(2)	173(2) K
Wavelength (Å)	0.71073	0.71073	0.71073	0.71073	0.71073
Crystal system	Triclinic	Monoclinic	Triclinic	Orthorhombic	Monoclinic
space group	P-1	P2(1)/c	P-1	Pbca	P2(1)/n
a (Å)	10.411(2)	10.557(2)	10.689(2)	13.118(3)	11.081(2)
b (Å)	13.111(3)	24.458(5)	10.696(2)	15.112(3)	18.089(4)
c (Å)	13.296(3)	13.624(3)	12.219(2)	25.481(5)	26.717(5)
α (°)	105.75(3)	90	75.64(3)	90	90
β (°)	105.04(3)	96.13(3)	69.97(3)	90	99.70(3)
γ (°)	95.57(3)	90	71.87(3)	90	90
Volume ($Å^3$)	1659.2(6)	3497.9(12)	1231.6(4)	5051.0(17)	5278.7(18)
Z	2	4	2	8	8
Dcalc(Mg m^{-3})	0.962	0.966	0.993	1.176	0.922
μ (mm^{-1})	0.082	0.081	0.094	1.675	0.087
F(000)	516	1096	388	1824	1536
Crystal size (mm)	0.18×0.16×0.14	0.28×0.26×0.22	0.20×0.20×0.20	0.39×0.26×0.07	0.28×0.26×0.22
θ range (°)	1.67–27.48	1.72–27.52	1.80–27.52	2.23–25.32	1.37–27.51

Limiting indices	$-13 \le h \le 12$, $-16 \le k \le 16$, $-17 \le l \le 17$	$-13 \le h \le 13$, $-31 \le k \le 30$, $-17 \le l \le 10$	$-13 \le h \le 12$, $-13 \le k \le 13$, $-15 \le l \le 11$	$-15 \le h \le 15$, $-17 \le k \le 14$, $-30 \le l \le 18$	$-14 \le h \le 14$, $-23 \le k \le 22$, $-34 \le l \le 34$
No. of rflns collected	14746	16452	10970	16634	35353
No. of unique rflns	7525	7972	5522	4577	11977
Rint	0.0968	0.0523	0.0336	0.0562	0.0715
Completeness to θ (%)	98.7 %	98.9 %	97.5 %	99.4 %	98.6 %
Goodness-of-fit on F^2	1.056	1.097	1.114	1.074	1.042
Final R indices [I>2σ (I)]	R1=0.1177, wR2=0.3079	R1=0.0896, wR2=0.2240	R1=0.0809, wR2=0.2300	R1=0.0861, wR2=0.2211	R1=0.0972, wR2=0.2554
R indices (all data)	R1=0.1711, wR2=0.3443	R1=0.1187, wR2=0.2429	R1=0.0926, wR2=0.2418	R1=0.1072, wR2=0.2372	R1=0.1344, wR2=0.2773
Largest diff peak hole (e $Å^{-3}$)	0.671, -0.352	0.317, -0.231	0.451, -0.339	1.380, -0.372	0.390, -0.384

3. Results and Discussion

*3.1. Synthesis and Characterization of Dialkylaluminium 2-Imidazolylphenolates (**C1**–**C11**).*

The organic compounds to be used as ligands (**L1–L9**) were prepared according to our previous procedure [55]. Subsequently, the stoichiometric reaction of the organic compounds (**L1**–**L9**) and AlR_3 (R = Me, Et and *i*Bu) were carried out in toluene at -20 °C, affording the corresponding dialkylaluminium 2-imidazolylphenolates (**C1**–**C11**, Scheme 1) in high yield; such reactions illustrate the inactivity of the *N*-H of the imidazole toward alkylaluminium. All the aluminium compounds were characterized by $^1H/^{13}C$ NMR spectroscopy and by elemental analyses. Comparison of the ^1H NMR spectra of **C1**–**C11** with those of the corresponding 'free' ligands **L1**–**L9** revealed a shift of the alkyl-resonances to the high-field region (δ -0.22 to -1.01 ppm), and the disappearance of the O–*H* signals of the free ligands. Moreover, a number of resonances in the range -7.7 to -9.6 ppm in ^{13}C NMR spectra of **C1**–**C11** were consistent with the existence of alkyl-Al bonds. To confirm their unambiguous molecular structures, single crystals of complexes **C1, C2, C4, C6** and **C11** were obtained from their toluene/*n*-heptane solutions at -20 °C. All aluminium complexes possessed a similar structure, namely distorted tetrahedron geometry at Al, and their molecular structures are shown in Figures 1–5; selected bond lengths and angles are tabulated in Table 2.

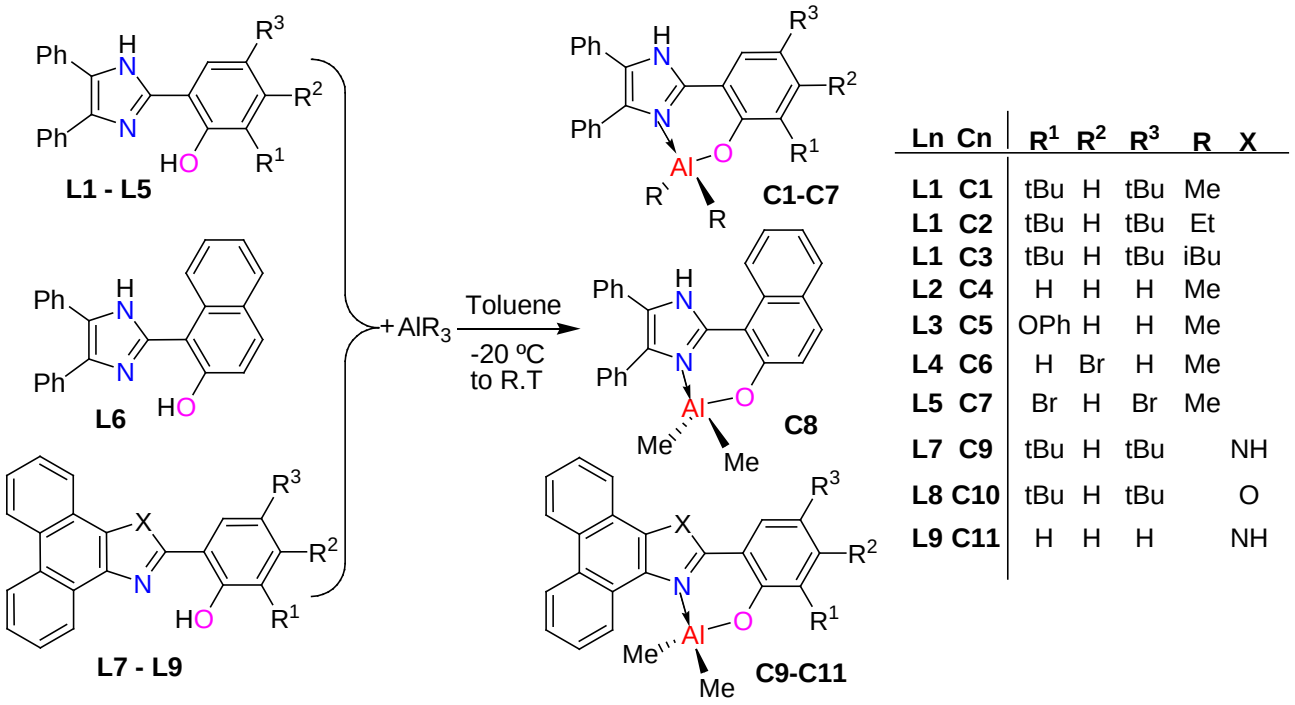

Ln	Cn	R^1	R^2	R^3	R	X
L1	C1	tBu	H	tBu	Me	
L1	C2	tBu	H	tBu	Et	
L1	C3	tBu	H	tBu	iBu	
L2	C4	H	H	H	Me	
L3	C5	OPh	H	H	Me	
L4	C6	H	Br	H	Me	
L5	C7	Br	H	Br	Me	
L7	C9	tBu	H	tBu		NH
L8	C10	tBu	H	tBu		O
L9	C11	H	H	H		NH

Scheme 1 Synthesis of the dialkylaluminium complexes **C1–C11**

Table 2. Selected bond length and bond angles

Complex	**C1**	**C2**	**C4**	**C6**	**C11**
		Bond length (Å)			
Al1-O1	1.779(3)	1.761(2)	1.764(2)	1.770(4)	1.798(3)
Al1-N1	1.953(3)	1.948(3)	1.947(2)	1.964(5)	1.954(3)
Al1-C22	1.961(5)	1.959(4)	1.962(3)	1.956(6)	1.974(4)
Al1-C23	1.955(5)	1.972(4)	1.962(4)	1.958(7)	1.965(4)
O1-C1	1.323(5)	1.328(3)	1.329(3)	1.329(8)	1.323(4)
N1-C7	1.328(5)	1.343(4)	1.344(3)	1.338(7)	1.326(4)
N1-C8	1.396(5)	1.388(4)	1.389(3)	1.382(7)	1.419(4)
		Bond angles (º)			
O(1)-Al(1)-N(1)	93.70(14)	92.82(11)	94.24(10)	93.8(2)	95.06(12)
O(1)-Al(1)-C(23)	113.21(18)	110.80(14)	113.36(15)	111.8(3)	110.14(16)
N(1)-Al(1)-C(23)	111.17(19)	110.38(13)	108.05(13)	112.5(3)	109.54(16)
O(1)-Al(1)-C(22)	109.5(2)	109.70(16)	109.68(14)	108.6(3)	110.91(16)
N(1)-Al(1)-C(22)	109.7(2)	113.06(15)	113.54(13)	108.1(3)	111.02(15)
C(23)-Al(1)-C(22)	117.1(2)	117.39(16)	115.97(17)	119.0(3)	117.82(17)
C(1)-O(1)-Al(1)	129.4(3)	134.6(2)	132.93(18)	129.2(4)	126.5(2)
C(7)-N(1)-C(8)	107.5(3)	107.2(2)	107.1(2)	107.3(4)	105.2(3)
C(7)-N(1)-Al(1)	119.7(3)	122.5(2)	123.04(17)	121.2(4)	121.0(2)

C(8)-N(1)-Al(1)	132.7(3)	129.7(2)	129.44(18)	131.5(4)	132.5(2)

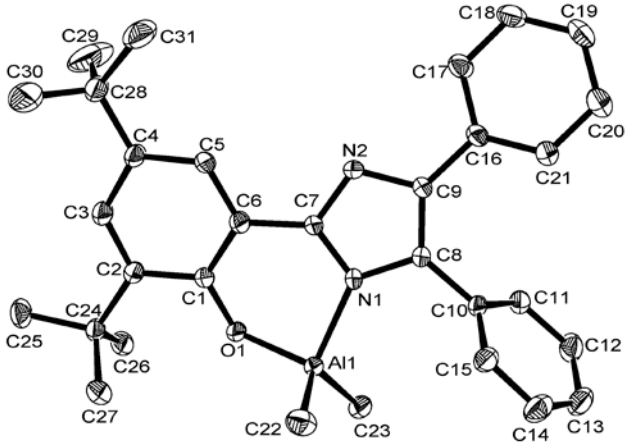

Figure 1 ORTEP drawing of **C1** with thermal ellipsoids drawn at the 30 % probability level. Hydrogen atoms are omitted for clarity.

As shown in **C1**, the Al center is coordinated through the N-atom and O-atom of the chelate ligand, similar coordination was observed for the zinc analogue [55]. The Al-C bond distances in **C1** are typical of σ-bonding at Al(1)-C(23) 1.955(5) Å, Al(1)-C(22) 1.961(5) Å. The Al(1)-O(1) bond [1.779(3) Å] is also a σ-bond, whilst the Al(1)-N(1) 1.953(3) Å is a coordination bond. Figure 2 depicts the structure of **C2**, which has a similar distorted tetrahedral geometry at aluminium as observed for **C1** (Figure 1), but with slight differences in the bond lengths and angles. For example, the bond lengths Al-N1 and Al-O1 [1.948(3) and 1.761(2) Å] are slightly shorter than those in **C1** [1.953(3) and 1.779(3) Å], whilst the bond lengths Al-C22 and Al-C23 in **C2** [1.959(4) and 1.972(4) Å] are longer than those in **C1** [1.961(5) and 1.955(5) Å]. Meanwhile, the bond angles of C(23)-Al(1)-C(22) and O(1)-Al(1)-N(1) are similar at 117.39(16) º and 92.82(11) º in **C2** versus 117.1(2) º and 93.70(14) º in **C1**, respectively.

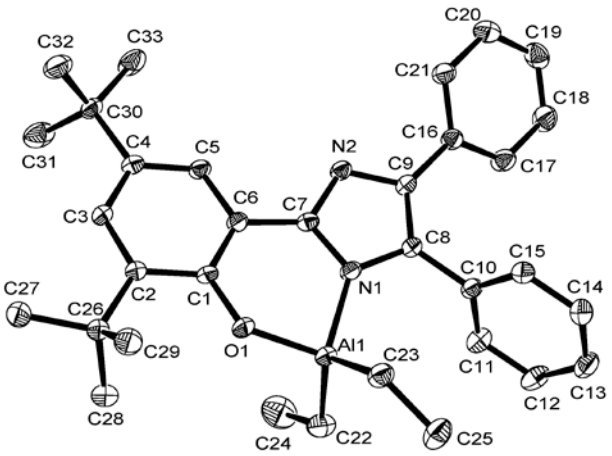

Figure 2 ORTEP drawing of **C2** with thermal ellipsoids drawn at the 30 % probability level. Hydrogen atoms are omitted for clarity.

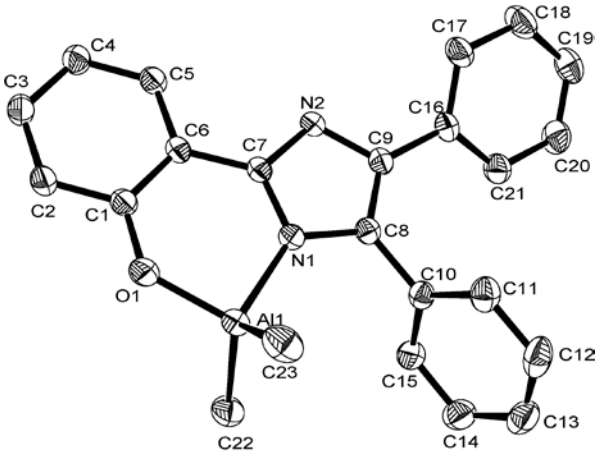

Figure 3. ORTEP drawing of **C4** with thermal ellipsoids drawn at the 30 % probability level. Hydrogen atoms are omitted for clarity.

As shown in Figure 3, the molecular structure of **C4**, which possesses a ligand without a substituent in the phenoxylate part of the chelate ligand, retains the same geometry as for the analogs **C1** and **C2,** but with slightly longer bond lengths for Al-C [1.962(3), 1.962(4)] versus **C1** [1.961(5), 1.955(5)], whilst the bond Al-O length (1.764(2) Å) is shorter than in **C1** (1.779(3) Å), suggestive of an electron donor effect on the structure. The *para*-bromo-phenoxylate complex **C6** (Figure 4) also possesses a distorted tetrahedral geometry, though the Al-N bond length [1.964(5) Å] is longer than that observed in **C1** [1.953(3) Å], **C2** [1.948(3) Å] and **C4** [1.947(2) Å]. Furthermore, the bond angles for O-Al-C in **C6** [111.8(3) º and 108.6(3) º] are smaller than those in **C1** [113.21(18) º and 109.5(2) º] and in **C4** [113.36(15) º and 109.68(14) º], which will contribute to different activity in the ring opening polymerization of lactides.

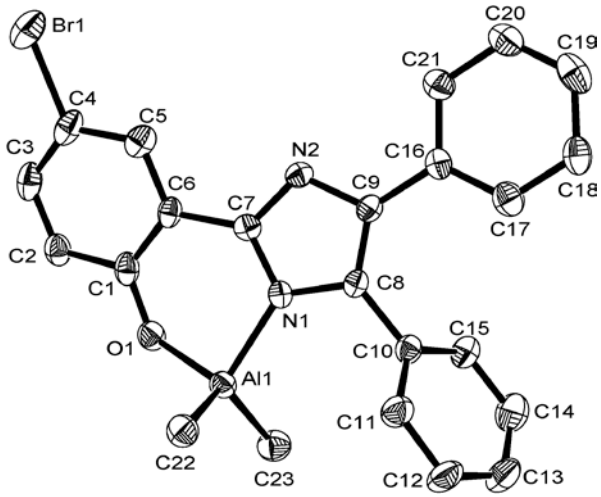

Figure 4. ORTEP drawing of **C6** with thermal ellipsoids drawn at the 30 % probability level. Hydrogen atoms are omitted for clarity.

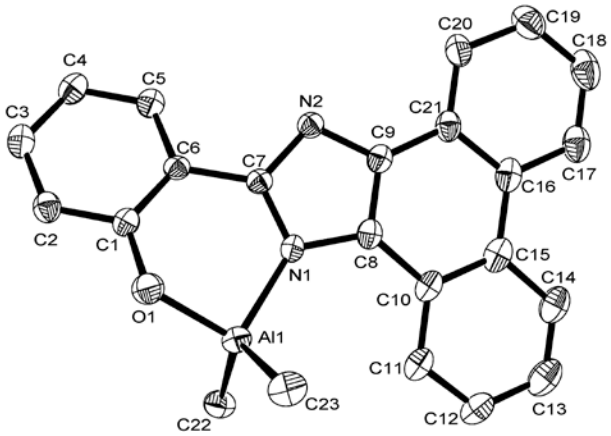

Figure 5. ORTEP drawing of **C11** with thermal ellipsoids drawn at the 30 % probability level. Hydrogen atoms are omitted for clarity. (Two independent molecules included, only one structure is listed)

By employing a phenanthroline moiety in place of the two phenyl groups on the imidazole, the resulting complex **C11** also exhibited a similar distorted tetrahedral geometry at aluminium (shown in Figure 5). The bond lengths of Al-C22, Al-C23, Al-O1 and Al-N1 in **C11** [1.974(4), 1.965(4), 1.798(3) and 1.954(3) Å] are much longer than those in **C4** [1.962(3), 1.962(4), 1.764(2), and 1.947(2) Å], suggesting that the constraint caused by the phenanthrolyl group results in non-symmetrical bonding between the aluminium and the two methyl groups.

3.2 Catalytic Behavior toward Ring Opening Polymerization (ROP) of Lactides (LA)

Alkylaluminium compounds are often reported as efficient catalysts for ring-opening polymerization (ROP) of cyclic esters [56-59]. Herein, we have investigated the catalytic behavior of **C1–C11** towards the ROP of lactides including *L*-lactide, *D*-lactide and *rac*-lactide.

Initially, the complex **C1** was employed to optimize the ROP conditions for *L*-lactide, and the results are collected in Table 3. An initial induction period was observed for the polymerization of *L*-lactide, consistent with other systems reported in the literature [14, 60]. It is noteworthy that the ROP of *L*-lactide by **C1** can proceed at elevated reaction temperatures, both with or without BnOH present; however, the activity is very low at temperatures lower than 90 ºC, (runs 1–4, Table 3). Using the molar ratio 250:1 of *L*-LA:Al, the higher the reaction temperature on going from 70 to 110 ºC, the better the efficiency of the ROP in both the presence of BnOH (runs 2, 4, 6) or absence of BnOH (runs 1, 3, 5). Prolonging the reaction time led to higher conversion rates (runs 5, 7, 9, 11 and runs 6, 8, 10, 12 in Table 3), and resulted in polymers with higher molecular weights. Increasing the *L*-LA:Al ratio resulted in a polymer with a higher molecular weight but wider polydispersity both in the presence of BnOH (runs 6, 14, 16) and without BnOH (runs 5, 13, 15) present. The values of M_n for the obtained polymer *vs* either the LA/Al molar ratios or the reaction time did not increased in parallel, indicating the nonlinearity of the reaction system. According to data in Table 3 (runs 5 *vs* 6, 7 *vs* 8, 11 *vs* 12, 13 *vs* 14, 15 *vs* 16), the catalytic system **C1** in the absence of BnOH produced polymer with much higher molecular weight and broader dispersity than did the **C1**/BnOH system. The molecular weights

observed for the PLAs were generally higher than their M_{ncal}, suggesting that the aluminium complexes are only partly acting as the initiators in the polymerization process.

Trials using different solvents such as THF, CH_2Cl_2 or *n*-heptane resulted in much lower efficiency (from trace to 28.1 %, runs 17–22 in Table 3) than when using toluene as solvent. Given the significant differences observed when using **C1** versus **C1**/BnOH, the ROP of lactides using **C2** – **C11** was further investigated, both in the presence and absence of BnOH, at 110 ºC over 24 h in toluene.

Table 3. The ROP of *L*-Lactide by **C1**[a]

Run	*L*-LA Al:BnOH	T/°C	Time (h)	Polymer(mg) /Conv. %))	$M_n \times 10^{-4}$ [b]	PDI
1	250:1:0	70	24	Trace		
2	250:1:1	70	24	Trace		
3	250:1:0	90	24	155 (43.1)		
4	250:1:1	90	24	172 (47.8)		
5	250:1:0	110	24	350 (98.2)	9.72	1.46
6	250:1:1	110	24	352 (97.7)	6.83	1.26
7	250:1:0	110	12	170 (47.2)	5.73	1.45
8	250:1:1	110	12	318 (88.3)	3.95	1.18
9	250:1:0	110	20	336 (93.3)		
10	250:1:1	110	20	345 (95.8)		
11	250:1:0	110	36	360 (100)	9.88	1.67
12	250:1:1	110	36	360 (100)	8.99	1.59
13	500:1:0	110	24	656 (91.1)	11.1	1.65
14	500:1:1	110	24	682 (94.7)	9.05	1.39
15	1000:1:0	110	24	902 (62.6)	10.8	1.82
16	1000:1:1	110	24	987 (68.5)	9.00	1.61
17[c]	250:1:0	66	24	trace		
18[c]	250:1:1	66	24	trace		
19[d]	250:1:0	40	24	45 (12.5)	1.62	1.06
20[d]	250:1:1	40	24	62 (17.2)	0.34	1.15
21[e]	250:1:0	98	24	trace		
22[e]	250:1:1	98	24	101 (28.1)	0.12	1.21

[a] Conditions: 10 μmol Al, 1.0 M *L*-LA toluene solution [b] GPC data in THF *vs*. polystyrene standards, using a correcting factor 0.58 [61]. [c] THF as solvent [d] CH_2Cl_2 as solvent [e] *n*-heptane as solvent

The ^{1}H NMR of the resultant polymer obtained via **C1**/BnOH (run 8, 20, 22, Table 3) clearly showed the signal of -OCH_2Ph (δ 7.34-7.33, 4.36-4.34 ppm) and –OCH_3 (δ 3.43, 3.75 ppm), suggesting that

Al-OCH_2Ph species initiated the ROP and formed the polymer-Al intermediate, which was subsequently quenched through reacting with methanol to form a terminal $–OCH_3$.

3.2.1. Ring Opening Polymerization of *L*, *D*, *Rac*-Lactides by the C1–C11/BnOH Systems

By employing the optimized conditions found for **C1**, the ring opening polymerization of lactides by the aluminium complexes **C1-C11** in the presence of one equivalent of BnOH was conducted and the results are collected in Table 4.

Table 4 Ring Opening Polymerization of Lactides by the **C1–C11**/BnOH Systems

		ROP of *L*-LA				ROP of *D*-LA				ROP of *Rac*-LA			
Run	Cat.	Polymer (mg)/Conv.(%)	M_n $\times10^{-4b}$	M_{ncal} $\times10^{-4b}$	PDI[b]	Polymer (mg)/Conv.(%)	M_n $\times10^{-4b}$	M_{ncal} $\times10^{-4b}$	PDI[b]	Polymer (mg)/Conv.(%)	M_n $\times10^{-4b}$	M_{ncal} $\times10^{-4b}$	PDI[b]
1	**C1**	352 (97.8)	7.63	3.56	1.26	360 (100)	11.2	3.61	1.36	360 (100)	3.88	3.61	1.87
2	**C2**	338 (93.9)	6.57	3.39	1.27	352 (97.8)	5.83	3.53	1.46	344 (95.6)	3.43	3.45	1.98
3	**C3**	323 (89.7)	5.77	3.24	1.38	340 (94.4)	4.64	3.41	1.47	338 (93.9)	2.56	3.39	2.48
4	**C4**	354 (98.3)	5.40	3.55	1.73	360 (100)	4.48	3.61	1.47	360 (100)	2.91	3.61	1.85
5	**C5**	325 (90.3)	5.81	3.26	1.09	291 (80.8)	5.10	2.92	1.55	201 (55.8)	2.97	2.02	1.55
6	**C6**	312 (86.7)	6.61	3.13	1.17	290 (80.6)	3.48	2.91	1.48	355 (98.6)	2.79	3.56	1.33
7	**C7**	347 (96.4)	5.66	3.48	1.52	332 (92.2)	4.20	3.33	1.53	360 (100)	2.97	3.61	1.57
8	**C8**	343 (95.3)	3.71	3.44	1.63	346 (96.1)	4.49	3.47	1.79	352 (97.8)	2.72	3.53	1.87
9	**C9**	356 (98.9)	6.57	3.57	1.39	358 (99.4)	3.84	3.59	1.57	351 (97.5)	3.24	3.52	1.77
10	**C10**	360 (100)	8.65	3.61	1.52	336 (93.3)	3.79	3.37	1.55	360 (100)	2.91	3.61	1.83
11	**C11**	336 (93.3)	5.81	3.37	1.47	310 (86.1)	3.11	3.11	1.58	340 (94.4)	3.34	3.41	1.54

[a] Conditions: 10 μmol Al, 360 mg (2.5 mmol) L-LA, 2.5 mL toluene, 110 °C, 24h. [b] GPC data in THF *vs*. polystyrene standards, using a correcting factor 0.58 [61].

Generally, these aluminium complexes exhibited moderate to good catalytic activity with conversion rates of 86.7 to 100 % for ROP of lactides. The results of the ROP of *L*-lactide and *D*-lactide showed that the resultant polymers have much a higher molecular weight than the calculated values based on a "living manner", suggesting that only parts of the aluminium complex formed the active species in the ROP of *L*-lactides. In contrast, the ROP of *rac*-lactides afforded lower molecular weights and a broader distribution of polymers than that for *L*-, *D*- lactides under the same conditions. In particular, the M_n of poly(*rac*-LA) were lower than the M_{ncal}, suggesting regeneration of the active Al-species occurred during the ROP process.

The significant influence exerted by the nature of the ligands was also seen in the ROP by these complexes. As shown in Table 4, the alkyl groups attaching to the Al center affected the catalytic efficiency and the molecular weight of the obtained polymers; the bulkier the alkyl group, the lower the conversion and the lower the molecular weight of the obtained PLA, which can be illustrated by the same decrease order for ROP of *L*-, *D*- and *Rac*-Lactides: **C1** (Me) > **C2** (Et) > **C3** (^{i}Bu) (runs 1–3 in Table 4). The initiators **C1, C4** and **C7** bearing analogous ligands show similar efficiency (runs 1, 4,

7 in Table 4), but the obtained polymers by **C4** possessed much higher molecular weights than those via **C1** and **C7**, which is presumably a consequence of the bulky *t*Bu substituents R^3 at the *ortho*-position of the phenolate suppressing the chain termination and transfer.

The other complexes screened exhibited different conversion yields, but can be regarded as highly efficient in most cases. The ligands containing the fused phenanthrene or the two phenyl groups on the imidazole performed with high efficiency, *ie* **C9** (98.9 %, 99.4 %, 97.5 %) and **C1** (97.8 %, 100 %, 100 %) for ROP of *L*-, *D*-, *Rac*-LA (run 1,4). In addition, **C9** exhibited a higher conversion rate than **C11** for the ROP of lactides (run 9, 11)**,** suggesting that the donor stronger ability of the ^{t}Bu *vs* H played an important role. Use of ligands with oxazole instead of imidazole were found to enhance the catalytic activity for ROP of *L*-, *Rac*-LA, but decreased the activity for *D*-LA (run 9, 10 in Table 4). Comparison of the ligand sets with either phenoxylate or naphthalenoxlate (runs 4 and 8 in Table 4) revealed that complex **C8** having the naphthalenoxlate moiety exhibited a slightly lower efficiency than did complex **C4** having the phenoxylate group. With an additional phenoxyl group (OPh) at the *ortho*-position of the phenoxylate, the complex **C5** exhibited lower activity than did **C4** for the ROP of lactides (runs 4 and 5 in Table 4).

It is worth mentioning that the obtained poly(*rac*-lactide)s were commonly amorphous, indicating poor stereo-selectivity for the ROP of lactides by these bi-dentate aluminium complexes. In their ^{1}H NMR spectra, the signals for $PhCH_2O$- were very weak in most cases for the PLA with high molecular weights, but selected PLA with relatively low molecular weights clearly showed the signal of $PhCH_2O$-.

3.2.2 Ring Opening Polymerization of Lactides by C1–C11

As shown in Table 3, the catalytic system using **C1** without benzyl alcohol produced PLAs with higher molecular weights than the systems employing **C1** with BnOH. In general, better mechanical properties are expected for PLAs with high molecular weights, therefore the ROP solely by the aluminium complexes **C1**-**C11** (without benzyl alcohol) was also investigated.

Run	Cat.	ROP of *L*-LA				ROP of *D*-LA				ROP of *Rac*-LA			
		Polymer (mg)/ conv.(%)	M_n $\times10^{-4b}$	M_{ncal} $\times10^{-4b}$	PDI[b]	Polymer (mg)/ conv.(%)	M_n $\times10^{-4b}$	M_{ncal} $\times10^{-4b}$	PDI[b]	Polymer (mg)/ conv.(%)	M_n $\times10^{-4b}$	M_{ncal} $\times10^{-4b}$	PDI[b]
1	**C1**	350 (98.2)	11.0	3.50	1.46	342 (95.0)	12.3	3.42	1.43	332 (92.2)	7.36	3.32	1.74
2	**C2**	346 (96.1)	8.10	3.46	1.52	336 (93.9)	9.93	3.36	1.49	289 (80.3)	5.96	2.89	1.76
3	**C3**	333 (92.5)	6.77	3.33	1.63	338 (93.3)	7.37	3.38	1.52	260 (72.2)	5.53	2.60	1.80
4	**C4**	352 (97.8)	8.97	3.52	1.77	332 (92.2)	6.85	3.32	1.65	358 (99.4)	6.56	3.58	1.47
5	**C5**	299 (83.1)	11.8	2.99	1.12	280 (77.8)	7.38	2.80	1.64	301 (83.6)	4.85	3.01	1.73
6	**C6**	308 (85.6)	3.30	3.08	3.45	276 (76.7)	4.28	2.76	2.24	344 (95.6)	6.29	3.44	1.46
7	**C7**	343 (95.3)	9.50	3.43	1.19	324 (90.0)	5.64	3.24	1.95	360 (100)	6.01	3.60	1.56
8	**C8**	339 (94.2)	5.64	3.39	1.91	342 (95.0)	5.22	3.42	2.49	351 (97.5)	5.67	3.51	1.61
9	**C9**	349 (96.9)	8.15	3.49	1.49	303 (84.2)	5.26	3.03	1.83	330 (91.7)	6.25	3.30	1.59
10	**C10**	360 (100)	12.1	3.60	1.79	312 (86.9)	5.53	3.12	1.71	360 (100)	5.31	3.60	1.72

11	**C11**	332 (92.2)	8.10	3.32	1.41	297 (82.5)	4.89	2.97	1.77	341 (94.7)	6.01	3.41	1.56

Table 5 Ring Opening Polymerization of Lactides by the **C1–C11**[a]

[a] Conditions: 10 μmol Al, 360 mg (2.5 mmol) L-LA, 2.5 mL toluene, 110 °C, 24 h. [b] GPC data in THF *vs*. polystyrene standards, using a correcting factor 0.58 [61].

Firstly, the ROP of *L*-lactide revealed good activities with conversion rates of 83.1 to 100 %, similar to the results by **C1**–**C11**/BnOH. The advantage of high molecular weight products from **C1**–**C11**/BnOH, is off-set by the observed wide molecular distributions (PDI = 1.19–3.45). The measured M_n data for the PLAs were much higher than the M_{ncal} data, probably being caused by deviation at the initiation stage, and consistent with established features for metal alkyl initiators [62, 63]. The influence of the ligands on the catalytic behavior of the complexes was similar to the results by **C1**–**C11**/BnOH. The conversion rates and molecular weights decreased in the order **C1** (Me, 98.2 %, M_n: 11.0×10^4) > **C2** (Et, 96.1 %, 8.10×10^4) > **C3** (*i*Bu, 92.5 %, 6.77×10^4) (runs 1–3, Table 5). Similar conversion rates were observed by **C1** (4,6-di*t*Bu, 98.2 %), C**4** (4,6-diH, 97.8 %) and **C7** (4,6-diBr, 95.3 %); **C9** (96.9 %) and **C11** (92.2 %); **C4** (97.8 %) and **C8** (94.2 %).

In the absence of BnOH, all aluminium complexes possessed relatively lower efficiency for the ROP of *D*-lactide (76.7 to 95.0 %), however, the resultant polymers showed much higher molecular weights than those obtained in the systems in the presence of BnOH. The nature of ligands with different substituents affected the catalytic behavior of their complexes with only a slight influence on their efficiencies as reflected by the conversion rates of *D*-lactide (93.3–95.0 %, runs 1–3, Table 5), however, polymers with lower molecular weight resulted from the systems bearing bulkier substituents (with the substituents as Me, Et, and *i*Bu, the data for molecular weights was 12.3, 9.93, and 7.37×10^4; runs 1–3, Table 5). In addition, the conversion rates of *D*-lactide slightly decreased in the order **C1** (4,6-di*t*Bu, 95.0 %) > **C4** (4,6-diH, 92.2 %) > **C7** (4,6-diBr, 90.0 %) and **C9** (*t*Bu, 84.2 %) > **C11** (H, 82.5 %), probably due to the stronger electron-donating substituents. Again, **C5** exhibited the lowest activity of this series.

Under the same conditions, aluminium complexes **C1-C11** could initiate the ROP of *Rac*-Lactide with conversion rates ranging from 72.2 % to 100 %. To the best of our knowledge, this is a rare example of alkylaluminium complexes acting as active initiators for the ROP of *rac*-lactide without a co-catalyst [64, 65]. Herein, the resultant polymers possessed higher molecular weights (M_n = 4.85 – 7.36×10^4) over the catalytic systems screened in the presence of BnOH ($2.56 – 3.88 \times 10^4$, Table 4). In terms of the ligand influence, the bulkiness of the Al-alkyl led to lower conversion rates and the obtaining polymers had lower molecular weights, as shown by the order: **C1** (Me, 92.2 %, 7.36×10^4) > **C2** (Et, 80.3 %, 5.96×10^4) > **C3** (*i*Bu, 72.2 %, 5.53×10^4) (runs 1–3 in Table 5). There was little difference observed for catalytic systems **C1**, **C4**–**C11** with conversion rates of 91.7 to 100 % and molecular weights of $5.31–7.36 \times 10^4$, the exception was **C5** with a low conversion rate of 83.6 % and a polymer with a molecular weight of 4.85×10^4 (run 5 in Table 5). All obtained poly(rac-lactides) were amorphous, indicating the poor selectivity by these bi-dentate aluminium complexes. This also indicated the poor stereo-selectivity during the ring opening polymerization. The MALDI-TOF spectra showed several series of peaks with the major peak as a macrocyclic polymer (residual 23, Na^+ adduct). The results are consistent with intra-molecular *trans*-esterification [66].

4. Conclusions

A series of dialkylaluminium diphenylimidazolylphenolate complexes (**C1–C11**) was synthesized and fully characterized by $^{1}H/^{13}C$ NMR spectroscopy and elemental analysis. The molecular structures of compounds **C1**, **C2**, **C4**, **C6** and **C11** were confirmed by single crystal X–ray diffraction and possess a similar distorted tetrahedral geometry at aluminium. These bi-dentate aluminium complexes exhibited high efficiency towards the ROP of *L*-lactide, *D*-lactide, *rac*-lactides, both in the presence or absence of BnOH. With the exception of the ROP of *rac*-lactide by **C1**-**C11**/BnOH which produced polymers with observed lower molecular weights than calculated results, most obtained PLA possessed higher molecular weights than their calculated data. The polymers obtained by the sole aluminium complexes (*ie* without benzyl alcohol) possessed higher molecular weight than those produced in the catalytic systems in the presence of BnOH, indicating that the BnOH acted as a chain transfer agent. The catalytic systems without BnOH present produced PLA as macrocyclic polymers, meanwhile catalytic systems in the presence of BnOH formed polymers with terminal BnO-. The nature of the ligands with various substituents affected the catalytic activities and obtained polymers.

Acknowledgments

This work was supported by National Natural Science Foundation of China (No. 20904059 and 51273202). The EPSRC are thanked for a travel grant (to CR).

References and Notes

1. Ikada, Y.; Tsuji, H. Biodegradable polyesters for medical and ecological applications. *Macromol. Rapid Commun.* **2000**, *21*, 117–132.
2. Winzenburg, G.; Schmidt, C.; Fuchs, S.; Kissel, T. Biodegradable polymers and their potential use in parenteral veterinary drug delivery systems. *Adv. Drug Deliv. Rev.* **2004**, *56*, 1453–1466.
3. Auras, R.; Harte, B.; Selke, S. An overview of polylactides as packaging materials. *Macromol. Biosci.***2004**, *4*, 835–864.
4. Vert, M.; Li, S.; Spenlehauer, G.; Guerin, P. Vert, M.; Li, S.; Spenlehauer, G.; Guerin, P. Bioresorbability and biocompatibility of aliphatic polyesters. *J. Mater. Sci., Mater. Med.* **1992**, *3*, 432–446.
5. Chiellini, E.; Solaro, R. Biodegradable polymeric materials. *Adv. Mater.* 1996, *8*, 305–313.
6. Swift, G. Directions for environmentally biodegradable polymer research. *Acc. Chem. Res.* **1993**, *26*, 105–110.
7. Kricheldorf, H. R.; Kreiser-Saunders: I.; Juergens, C.; Wolter, D. Polylactides - synthesis, characterization and medical application. *Macromol. Symp.* **1996**, *103*, 85–102.
8. Ikada, Y.; Tsuji, H. Biodegradable polyesters for medical and ecolpgical applications. *Macromol. Rapid Commun.* **2000**, *21*, 117–132.

9. Van Hummel, G. J.; Harkema, S.; Kohn, F. E.; Feijen, J. Structure of 3,6-dimethyl-1,4-dioxane-2,5-dione [D-,D-(L-,L-)lactide]. *Acta Crys. B*, **1982**, *38*, 1679–1681.
10. Chisholm, M. H.; Eilerts, N. W.; Huffman, J. C.; Iyer, S. S.; Pacold, M.; Phomphrai, K. Molecular design of single-site metal alkoxide catalyst precursors for ring-opening polymerization reactions leading to polyoxygenates. 1. Polylactide formation by achiral and chiral magnesium and zinc alkoxides, (η3-L)MOR, where L = trispyrazolyl- and trisindazolylborate Ligands. *J. Am. Chem. Soc.* **2000**, *122*, 11845–11854.
11. Thomas, C. M. Stereocontrolled ring-opening polymerization of cyclic esters: synthesis of new polyester microstructure. *Chem. Soc. Rev*., **2010**, *39*, 165–173.
12. Robert, C.; de Montigny, F.; Thomas, C. M. Tandem synthesis of alternating polyesters from renewable resources. *Nat. Commun*., **2011**, *2*, 586.
13. Dijkstra, P.J.; Du, H.; Feijen, J. Single site catalysts for stereoselective ring-opening polymerization of lactides. *Polym. Chem*., **2011**, *2*, 520–527.
14. Matsubara, K.; Terata, C,; Sekine, H.; Yamatani, K.; Harada,T.; Eda, K.; Dan, M.; Koga, Y.; Yasuniwa, M. Stereoselective ring-opening polymerization of D,L-lactide, initiated by aluminum isopropoxides bearing tridentate nonchiral schiff-base Ligands. *J. Polym. Sci., Polym. Chem.* **2012**, *50*, 957–966.
15. Kowalski, A.; Duda, A.; Penczek, S. Polymerization of L, L-Lactide initiated by aluminum isopropoxide trimer or tetramer. *Macromolecules* **1998**, *31*, 2114–2122.
16. Li, C.-Y.; Tsai, C.-Y.; Lin, C.-H.; Ko, B.-T. Synthesis, structural characterization and reactivity of aluminium complexes supported by benzotriazole phenoxide ligands: air-stable alumoxane as an efficient catalyst for ring-opening polymerization of L-lactide. *Dalton Trans.*, **2011**, *40*, 1880–1887.
17. Ma, W.-A,; Wang Z.-X. Zinc and Aluminum complexes supported by quinoline-based N,N,N-chelate ligands: Synthesis, characterization, and catalysis in the ring-opening polymerization of ε-caprolactone and rac-lactide. *Organometallics*, **2011**, *30*, 4364–4373.
18. Whitelaw, E. L., Loraine, G.; Mahon, M. F.; Jones, M. D. Salalen aluminium complexes and their exploitation for the ring opening polymerisation of rac-lactide. *Dalton Trans.*, **2011**, *40*, 11469–11473.
19. Bouyahyi, M.; Roisnel, T.; Carpentier, J. F. Aluminum complexes of bidentate fluorinated alkoxy-imino ligands: Syntheses, structures, and use in ring-opening polymerization of cyclic esters. *Organometallics*, **2012**, *31*, 1458–1466.
20. Spassky, N.; Wisniewski, M.; Pluta, C.; LeBorgne, A. A. Highly stereoelective polymerization of rac- (d,l)-lactide with a chiral Schiff's base/aluminum alkoxide initiator. *Macromol. Chem. Phys.* **1996**, *197*, 2627–2637.
21. Dechy-Cabaret, O.; Martin-Vaca, B.; Bourissou, D. Controlled ring-opening polymerization of lactide and glycolide. *Chem. Rev.* **2004**, *104*, 6147–6176.
22. O'Keefe, B. J.; Hillmyer, M. A.; Tolman, W. B. Polymerization of lactide and related cyclic esters by discrete metal complexes. *J. Chem. Soc., Dalton Trans.* 2001, 2215–2224.
23. Wu, J.-C.; Yu, T.-L.; Chen, C.-T.; Lin, C.-C. Recent developments in main group metal complexes catalyzed/initiated polymerization of lactides and related cyclic esters. *Coord. Chem. Rev.* 2006, *250*, 602–626.

24. Tschan, M. J.-L.; Brulé, E.; Haquette, P.; Thomas, C. M. Synthesis of biodegradable polymers from renewable resources. *Polym. Chem.*, **2012**, *3*, 836–851.
25. Stanford, M. J.; Dove, A. P. Stereocontrolled ring-opening polymerisation of lactide. *Chem. Soc. Rev*., 2010, *39*, 486–494.
26. Bhaw-Luximon, A.; Jhurry, D.; Spassky, N. Controlled polymerization of D,L-lactide using a Schiff's base Al-alkoxide initiator derived from 2-hydroxyacetophenone. *Polym. Bull.* **2000**, *44*, 31–38.
27. Jhurry, D.; Bhaw-Luximon, A.; Spassky, N. Synthesis of polylactides by new Al-Schiff's base complexes. *Macromol.Symp.* **2001**, *175*, 67–79.
28. Tang, Z.; Chen, X.; Yang, Y.; Pang, X.; Sun, J.; Zhang, X.; Jing, X. Stereoselective polymerization of rac-lactide with a bulky aluminum/Schiff base complex. *J. Polym. Sci., Polym. Chem.* **2004**, *42*, 5974–5982.
29. Nomura, N.; Ishii, R.; Yamamoto, Y.; Kondo, T. Stereoselective ring-opening polymerization of a racemic lactide by using achiral salen– and homosalen–aluminum complexes. *Chem. Eur. J.* **2007**, *13*, 4433–4451.
30. Ovitt, T. M.; Coates, G. W. Stereoselective ring-opening polymerization of rac-lactide with a single-site, racemic aluminum alkoxide catalyst: Synthesis of stereoblock poly(lactic acid). *J. Polym. Sci., Polym. Chem.* **2000**, *38*, 4686–4692.
31. Ovitt, T. M.; Coates, G. W. Stereochemistry of lactide polymerization with chiral catalysts: new opportunities for stereocontrol using polymer exchange mechanisms. *J. Am. Chem. Soc.***2002**, *124*, 1316–1326.
32. Zhong, Z.; Dijkstra, P. J.; Feijen, J. [(salen)Al]-Mediated, Controlled and Stereoselective Ring-Opening Polymerization of Lactide in Solution and without Solvent: Synthesis of Highly Isotactic Polylactide Stereocopolymers from Racemic d,l-Lactide. *Angew. Chem., Int. Ed.* **2002**, *41*, 4510–4513.
33. Zhong, Z.; Dijkstra, P. J.; Feijen, J. Controlled and Stereoselective Polymerization of Lactide: Kinetics, Selectivity, and Microstructures. *J. Am. Chem. Soc.* **2003**, *125*, 11291–11298.
34. Hormnirum, P.; Marshall, E. L.; Gibson, V. C.; Pugh, R. I.; White, A. J. P. Study of ligand substituent effects on the rate and stereoselectivity of lactide polymerization using aluminum salen-type initiators. *Proc. Natl. Acad. Sci. U.S.A.* **2006**, *103*, 15343–15348.
35. Du, H.; Pang, X.; Yu, H.; Zhuang, X.; Chen, X.; Cui, D.; Wang, X.; Jing, X. Polymerization of rac-lactide using schiff base aluminum catalysts: structure, activity, and stereoselectivity. *Macromolecules* **2007**, *40*, 1904–1913.
36. Nomura, N.; Ishii, R.; Akakura, M.; Aoi, K. J. Stereoselective ring-opening polymerization of racemic lactide using aluminum-achiral ligand complexes: exploration of a chain-end control mechanism. *J. Am. Chem. Soc.* 2002, *124*, 5938–5939.
37. Ishii, R.; Nomura, N.; Kondo, T. Stereoselective bulk polymerization of racemic lactide for stereoblock poly(racemic lactide) using an achiral aluminum complex. *Polym. J.* **2004**, *36*, 261–264.
38. Tang, Z.; Chen, X.; Pang, X.; Yang, Y.; Zhang, X.; Jing, X. Stereoselective Polymerization of rac-Lactide Using a Monoethylaluminum Schiff Base Complex. *Biomacromolecules* **2004**, *5*, 965–970.

39. Pappalardo, D.; Annunziata, L.; Pellecchia C. Living ring-opening homo- and copolymerization of ε-caprolactone and L- and D,L-lactides by dimethyl(salicylaldiminato)aluminum compounds. *Macromolecules* **2009**, *42*, 6056–6062.
40. Chisholm, M. H.; Lin, C.-C.; Gallucci, J. C.; Ko, B.-T. Binolate complexes of lithium, zinc, aluminium, and titanium; preparations, structures, and studies of lactide polymerization. *Dalton Trans* **2003**, 406–412.
41. Silvestri, A.; Grisi, F.; Milione, S. Ring opening polymerization of lactide promoted by alcoholyzed heteroscorpionate aluminum complexes. *J. Polym. Sci. Part A: Polym. Chem.* **2010**, *48*, 3632–3639.
42. Zhang, W.; Wang, Y.; Sun, W.-H.; Wang, L.; Redshaw C. Dimethylaluminium aldiminophenolates: synthesis, characterization and ring-opening polymerization behavior towards lactides. *Dalton Trans.* **2012**, *41*, 11587–11591.
43. Koller, J.; Bergman, R. G. Highly efficient aluminum-catalyzed ring-opening polymerization of cyclic carbonates, lactones, and lactides, including a unique crystallographic snapshot of an Intermediate. *Organometallics* **2011**, *30*, 3217–3224.
44. Yao, W.; Mu, Y.; Gao A., Gao, W.; Ye, L. Bimetallic anilido-aldimine Al or Zn complexes for efficient ring-opening polymerization of ε-caprolactone. *Dalton Trans.*, **2008**, 3199–3206.
45. Chakraborty D., Chen E. Y. X. Neutral, three-coordinate, chelating diamide aluminum complexes: catalysts/initiators for synthesis of telechelic oligomers and high polymers. *Organometallics*, **2002**, *21*, 1438–1442.
46. Chai Z. Y., Zhang C., Wang Z. X. Synthesis, characterization, and catalysis in ε-caprolactone polymerization of aluminum and zinc complexes supported by N,N,N-Chelate ligands. *Organometallics* **2008**, *27*, 1626–1633.
47. Shen, M.; Zhang, W.; Nomura, K.; Sun, W.-H. Synthesis and characterization of organoaluminum compounds containing quinolin-8-amine derivatives and their catalytic behaviour for ring-opening polymerization of e-caprolactone. *Dalton Trans.***2009**, 9000–9009.
48. Shen, M.; Huang, W.; Zhang, W.; Hao, X.; Sun, W.-H.; Redshaw, C. Synthesis and characterisation of alkylaluminium benzimidazolates and their use in the ring-opening polymerisation ofe-caprolactone. *Dalton Trans.* **2010**, 39, 9912–9922.
49. Liu, Z.; Gao, W.; Zhang, J.; Cui, D.; Wu, Q.; Mu, Y. bis(imino)aryl NCN pincer aluminum and zinc complexes: Synthesis, characterization, and catalysis on L-Lactide polymerization. *Organometallics* **2010**, 29, 5783–5790.
50. Zhang, C.; Wang, Z.-X. N, O-chelate aluminum and zinc complexes: synthesis and catalysis in the ring-opening polymerization of ε-caprolactone. *Appl. Organometal.Chem.***2009**, 23, 9–18.
51. Zhang, W.; Wang, Y.; Cao, J.; Wang L.; Pan, Y.; Redshaw, C.; Sun, W.-H. Synthesis and characterization of dialkylaluminum amidates and their ring-opening polymerization of ε-caprolactone. *Organometallics***2011**, *30*, 6253–6261.
52. Ma, W.-A.; Wang, L.; Wang, Z.-X. Dimethylaluminium iminophosphoranylenamides and iminophosphoranylanilides: Synthesis, characterisation, and their controlled ring-opening polymerisation of e-caprolactone. *Dalton Trans.***2011**, *40*, 4669–4677.
53. Alkarekshi,W.; Armitage, A. P.; Boyron, O.; Davies, C. J.; Govere, M.; Gregory, A.; Singh, K.; Solan, G. A. Phenolate substituent effects on ring-opening polymerization of ε‑caprolactone by

aluminum complexes bearing 2‐(phenyl-2-olate)-6-(1-amidoalkyl)pyridine pincers. *Organometallics* **2013**, *32*, 249–259.

54. Sheldrick, G. M. SHELXTL-97, Program for the Refinement of Crystal Structures; University of Göttingen: Göttingen, Germany, 1997.
55. Eseola, A. O.; Li, W.; Gao, R.; Zhang M.; Hao, X.; Liang, T.; Obi-Egbedi, N.O.; Sun, W.-H. Syntheses, structures, and fluorescent properties of 2-(1H-Imidazol-2-yl)phenols and their neutral Zn(II) complexes. *Inorg. Chem.***2009**, *48*, 9133–9146.
56. Chisholm, M. H.; Navarro-Llobet, D.; Simonsick, W. J., A comparative study in the ring-opening polymerization of lactides and propylene oxide. *Macromolecules* **2001**, *34*, 8851–8857.
57. Huang, C.-H.; Wang, F.-C.; Ko, B.-T.; Yu, T.-L.; Lin, C.-C. Ring-opening polymerization of ε-caprolactone and L-Lactide using aluminum thiolates as initiator. *Macromolecules* **2001**, *34*, 356–361.
58. Huang, W.-Y.; Chuang, S.-J.; Chunag, N.-T.; Hsiao, Datta, C.-S. A.; Chen, S.-J.; Hu, C.-H.; Huang, J.-H.; Lee, T.-Y.; Lin, C.-H. Aluminium complexes containing bidentate and symmetrical tridentate pincer type pyrrolyl ligands: synthesis, reactions and ring opening polymerization. *Dalton Trans.*, **2011**, *40*, 7423–7433.
59. Li, W.; Wu, W.; Wang, Y.; Yao, Y.; Zhang, Y.; Shen Q. Bimetallic aluminum alkyl complexes as highly active initiators for the polymerization of□-caprolactone. *Dalton Trans.*, **2011**, *40*, 11378–11381.
60. Jacobs, C.; Dubois, Ph.; Jerome, R.; Teyssie, Ph. Macromolecular engineering of polylactones and polylactides. 5. Synthesis and characterization of diblock copolymers based on poly-ε-caprolactone and PO~Y(L,L or D,L)lactide by aluminum alkoxides. *Macromolecules* **1991**, *24*, 3027–3034
61. Save, M.; Schappacher, M.; Soum, A. Controlled ring-opening polymerization of lactones and lactides initiated by lanthanum isopropoxide. I. General aspects and kinetics. *Macromol. Chem. Phys.* **2002**, *203*, 889–899.
62. Alonso-Moreno, C.; Garcés, A.; Sánchez-Barba, L. F.; Fajardo, M.; Fern-andez-Baeza, J.; Otero, A.; Antiñolo, A.; Lara-Sánchez, A.; López-Solera, I. Discrete heteroscorpionate lithium and zinc alkyl complexes. synthesis, structural studies, and ROP of cyclic esters. *Organometallics* **2008,** *27*, 1310–1321.
63. Chamberlain, B.; Cheng, M.; Moore, D.; Ovitt, T.; Lobkovsky, E.; Coates, G. W. Polymerization of lactide with zinc and magnesium α-diiminate complexes: stereocontrol and mechanism. *J. Am. Chem. Soc.* **2001**, *123*, 3229–3238.
64. Dunne, J. F.; Manna, K.; Wiench, J. W.; Ellern, A.; Pruski, M.; Sadow, A. D. Bis(oxazolinyl)phenylborane: a lewis acid-containing ligand for methide abstraction-based coordination to aluminum(III). *Dalton Trans.* **2010**, *39*, 641–653.
65. Otero, A.; Lara-Sanchez, A.; Fernandez-Baeza, J.; Alonso-Moreno, C.; Castro-Osma, J. A., Marquez-Segovia, I.; Sanchez-Barba, L. F.; Rodríguez, A.M.; Garcia-Martinez , J. C. Neutral and cationic aluminum complexes supported by acetamidate and thioacetamidate heteroscorpionate ligands as initiators for ring-opening polymerization of cyclic esters. *Organometallics* **2011**, *30*, 1507–1522.

66. Oledzka, E. Synthesis of genistein-containing star-shaped homo- and copolyesters by the ring-opening polymerization. *Polym. Bull.*, **2013**, DOI 10.1007/s00289-013-0973-5